NSF/CBMS Regional Conference in the Mathematical Sciences
College Station, TX 77843, May 18–22, 2009

ADAPTIVE FINITE ELEMENT METHODS FOR PARTIAL DIFFERENTIAL EQUATIONS

Rolf Rannacher
Institute of Applied Mathematics
University of Heidelberg
http://numerik.iwr.uni-heidelberg.de

Exercises

Lecture 1. Basic concepts of adaptivity
Lecture 2. Galerkin finite element method

Exercise 0: Develop formulas for determining the convergence rates $\mathcal{O}(h^\alpha)$ in computing functional values $J(u_h)$ on sequences of uniformly refined meshes for the case

(i) that the exact value $J(u)$ is known, and

(ii) that the exact value is not known.

Solution: The underlying assumption is that the error in the functional behaves regularly in h:

$$J(u) - J(u_h) = h^\alpha + o(h^\alpha).$$

(i) Suppose that the valus $J(u)$ is known. Then from the asymptotic assumption

$$|J(u) - J(u_h)| = h^\alpha, \quad |J(u) - J(u_{h/2})| = (h/2)^\alpha$$

we get

$$\Big|\frac{J(u) - J(u_h)}{J(u) - J(u_{h/2})}\Big| = 2^\alpha \qquad \Rightarrow \qquad \alpha = \log(2)^{-1} \log\Big(\Big|\frac{J(u) - J(u_h)}{J(u) - J(u_{h/2})}\Big|\Big).$$

(ii) If the value $J(u)$ is unknown, we may use the asymptotic assumption for three discrete solutions u_h, $u_{h/2}$ and $u_{h/4}$ obtained on three successive meshes of width h, $h/2$ and $h/4$, respectively,

$$J(u) - J(u_h) = h^\alpha, \quad J(u) - J(u_{h/2}) = (h/2)^\alpha, \quad J(u) - J(u_{h/4}) = (h/4)^\alpha$$

Consequently,

$$\begin{aligned} J(u_{h/2}) - J(u_h) &= h^\alpha - (h/2)^\alpha = h^\alpha(1 - (1/2)^\alpha) \\ J(u_{h/4}) - J(u_{h/2}) &= (h/2)^\alpha - (h/4)^\alpha = (h/2)^\alpha(1 - (1/2)^\alpha) \end{aligned}$$

and therefore,

$$\frac{J(u_{h/2}) - J(u_h)}{J(u_{h/4}) - J(u_{h/2})} = 2^\alpha \qquad \Rightarrow \qquad \alpha = \log(2)^{-1} \log\Big(\Big|\frac{J(u_{h/2}) - J(u_h)}{J(u_{h/4}) - J(u_{h/2})}\Big|\Big).$$

Exercise 1: Repeat the derivation of the "energy-norm" error estimate

$$\|\nabla e\| \le c_I c_S \Big(\sum_{K\in\mathbb{T}_h} h_K^2 \big\{ \|f + \Delta u_h\|_K^2 + \tfrac{1}{2} h_K^{-1} \|[\partial_n u_h]\|_{\partial K}^2 \big\} \Big)^{1/2}$$

($c_S = 1$) for the FE approximation of the boundary value problem

$$-\Delta u = f \quad \text{in } \Omega, \quad u|_{\partial\Omega} = 0,$$

by using (i) the coercivity of the problem or (ii) a duality argument.

Solution: (i) By coercivity and Galerkin orthogonality, we have

$$(\nabla e, \nabla e) = (\nabla(u - u_h), \nabla(e - \varphi_h)) = (f, e - \varphi_h) - (\nabla u_h, \nabla(e - \varphi_h))$$

for arbitrary $\varphi_h \in V_h$. Then, by the usual localization argument,

$$\begin{aligned} \|\nabla e\|^2 &= \sum_{K\in\mathbb{T}_h} \big\{ (f + \Delta u_h, e - \varphi_h) - \tfrac{1}{2}([\partial_n u_h], e - \varphi_h)_{\partial K} \big\} \\ &\le \Big(\sum_{K\in\mathbb{T}_h} h_K^2 \big\{ \|f + \Delta u_h\|_K^2 + \tfrac{1}{2} h_K^{-1} \|[\partial_n u_h]\|_{\partial K}^2 \big\} \Big)^{1/2} \\ &\quad \Big(\sum_{K\in\mathbb{T}_h} h_K^{-2} \big\{ \|e - \varphi_h\|_K^2 + \tfrac{1}{2} h_K \|e - \varphi_h\|_{\partial K}^2 \big\} \Big)^{1/2} \end{aligned}$$

Choose φ_h as the "Clement interpolation (generalized H^1 stable nodal interpolation) satisfying

$$\|e - \varphi_h\|_K^2 + \tfrac{1}{2} h_K \|e - \varphi_h\|_{\partial K}^2 \le c_I^2 h_K^2 \|\nabla e\|_{\tilde{K}}^2$$

for cell patches $\tilde{K} := \cup\{K' \in \mathbb{T}_h,\, K' \cap K \neq \emptyset\}$. From this, we conclude

$$\|e\|_E^2 \le \tilde{c}_I \Big(\sum_{K\in\mathbb{T}_h} h_K^2 \big\{ \|f + \Delta u_h\|_K^2 + \tfrac{1}{2} h_K^{-1} \|[\partial_n u_h]\|_{\partial K}^2 \big\} \Big)^{1/2} \|\nabla e\|$$

which implies the asserted estimate.
(ii) To obtain the same result via a duality argument, we consider the auxiliary problem

$$(\nabla\psi, \nabla z) = (\nabla\psi, \nabla e) \quad \forall \psi \in H_0^1(\Omega),$$

for $z \in H_0^1(\Omega)$, such that $(\nabla e, \nabla z) = \|\nabla e\|^2$. Obviously, $z = e$ in this case. Now the argument proceeds almost exactly as in (i).

Exercise 2: (i) Formulate the boundary value problem

$$-\alpha\Delta u + \vec{\beta}\cdot\nabla u + \gamma u = f \quad \text{in } \Omega, \quad u_{|\partial\Omega} = 0,$$

with constant coefficients, satisfying $\alpha > 0$, in variational form and give its dual problem corresponding to the error functional

$$J(u) := \int_\Omega u\, dx.$$

(ii) Derive the residual-based a posteriori error representation for this functional.

Solution: The variational formulation seeks $u \in H_0^1(\Omega)$ such that

$$a(u,\psi) := \alpha(\nabla u, \nabla\psi) + (\vec{\beta}\cdot\nabla u, \psi) + (\gamma u, \psi) = (f,\psi) \quad \forall\psi \in H_0^1(\Omega)$$

The corresponding dual probnlem in weak form seeks $z \in H_0^1(\Omega)$ such that

$$a(\varphi, z) = (\varphi, 1) \quad \varphi \in H_0^1(\Omega)$$

Observing $(\vec{\beta}\cdot\nabla\varphi, z) = -(\varphi, \vec{\beta}\cdot\nabla z)$, we obtain the weak dual problem

$$\alpha(\nabla\varphi, \nabla z) - (\varphi, \vec{\beta}\cdot\nabla z) + (\gamma\varphi, z) = (\varphi, 1)$$

or in strong form

$$-\alpha\Delta z - \vec{\beta}\cdot\nabla z + \gamma z = 1.$$

Exercise 3: Formulate the dual problem for the system

$$\begin{aligned} -\Delta u + v &= f \\ -\Delta v - w &= g \\ \vec{\beta} \cdot \nabla w + u + v &= 0, \end{aligned}$$

on a domain $\Omega \in \mathbb{R}^d$ with homogeneous Dirichlet boundary conditions $u = v = 0$ on $\partial\Omega$ and $w = 0$ on $\partial\Omega_{\text{in}}$, corresponding to the computation of the weighted average

$$J(\{u, v, w\}) := (v, \eta).$$

Solution: The variational formulation of the system is

$$A(\{u, v, w\}, \{\varphi, \psi, \xi\}) = F(\{\varphi, \psi, \xi\}) \quad \forall \{\varphi, \psi, \xi\} \in V,$$

with the "energy" form $A(\cdot, \cdot)$ and the functional $F(\cdot)$, for $X = \{u, v, w\}$ and $Y = \{\varphi, \psi, \xi\}$,

$$\begin{aligned} A(X, Y) &:= (\nabla u, \nabla \varphi) + (v, \varphi) + (\nabla v, \nabla \psi) - (w, \psi) + (\vec{\beta} \cdot \nabla w + u + v, \xi) \\ F(Y) &:= (f, \varphi) + (g, \psi), \end{aligned}$$

defined on the space

$$V := H_0^1(\Omega) \times H_0^1(\Omega) \times H_0^1(\Omega; \partial\Omega_{\text{in}}).$$

The dual solution $Z = \{x, y, z\}$ is determined by the dual problem

$$A^*(Z, Y) := A(Y, Z) = J(Y) \quad \forall Y \in V,$$

or written out:

$$(\nabla \varphi, \nabla x) + (\psi, x) + (\nabla \psi, \nabla y) - (\xi, y) + (\vec{\beta} \cdot \nabla \xi + \varphi + \psi, z) = (\psi, \eta)$$

This is equivalent to the system

$$\begin{aligned} (\nabla \varphi, \nabla x) + (\varphi, z) &= 0 \\ (\psi, x) + (\nabla \psi, \nabla y) + (\psi, z) &= (\psi, \eta) \\ -(\xi, y) - (\xi, \vec{\beta} \cdot \nabla z) &= 0, \end{aligned}$$

or strong form

$$\begin{aligned} -\Delta x + z &= 0 \\ x - \Delta y + z &= \eta \\ -y - \vec{\beta} \cdot \nabla z &= 0. \end{aligned}$$

Exercise 4 (Practical exercise): Hanging nodes are commonly used to ease mesh refinement and coarsening in triangular or quadrilateral meshes. However, the presence of hanging nodes (and also transition cells) usually destroys the uniformity pattern of the mesh which may drastically reduce the accuracy of approximation. To demonstrate this, consider the model Poisson problem

$$-\Delta u = f \ \text{ in } \Omega, \quad u_{|\partial\Omega} = 0,$$

on $\Omega = (-1,1)^2$, with right-hand side $f(x) = \frac{1}{2}\pi^2 \cos(\frac{1}{2}x_1\pi)\cos(\frac{1}{2}x_2\pi)$ and corresponding exact solution $u(x) = \cos(\frac{1}{2}x_1\pi)\cos(\frac{1}{2}x_2\pi)$. Compute the point-value $\partial_1 u(0.5, 0.5)$ and the boundary integral $J(u) = \int_{-1}^{1} \partial_n u(1,y)dy$ on a sequence of

a) uniform meshes with mesh-sizes $h = 2^{-1}$, $i = 1, 2, \ldots$;

b) refined meshes of approximately the same mesh complexity (or alternatively using the a posteriori error estimator and the corresponding refinement strategy presented in the course).

Compare the achieved accuracy.

Solution: a) Figure 1 shows the numerically computed approximation of the second derivatives for grids generated for the two functionals given in the exercise. Initially, the formula gives cell-wise constant values, but since this is a quantity that leads to poorly visible graphics, we generate a function where the value at each vertex is the mean value of the cell-wise quantities on the adjacent cells.

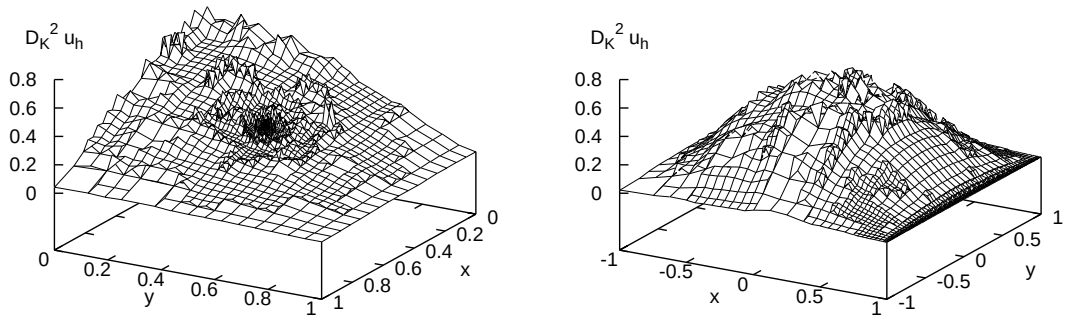

Figure 1: *$D_K^2 u_h$ on parts of optimal meshes generated by the dual weighted error estimator for $J(u) = \partial_1 u(a)$ (left) and $J(u) = \int_{-1}^{1} \partial_n u(1,y)dy$ (right).*

It can be seen that the result is a relatively smooth function except for those cells with hanging nodes. At these, the computed value is larger than on patches of uniform grids, and the ratio with the value of the second derivative of the exact solution does not converge to one. However, computing on a sequence of successively finer grids, the maximal value of the approximation to the second derivatives remains bounded for both examples.
b) For the regular solution, the same holds as said above for the quotient of the computed approximation of the second derivative with the asymptotic exact second derivatives,

shown in Figure 2. Again, the values remain bounded, but are irregular at cells with hanging nodes.

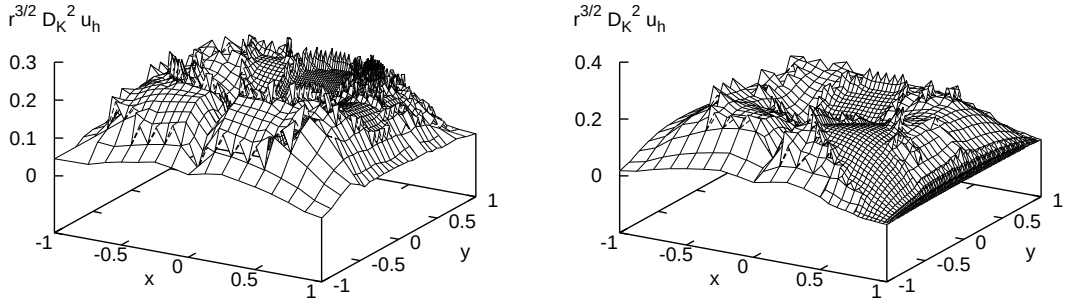

Figure 2: $\tilde{D}_K^2 u_h$ *on optimal meshes generated by the weighted error estimator for computing* $J(u) = \partial_1 u(a)$ *(left) and* $J(u) = \int_{-1}^{1} \partial_n u(1, y)\, dy$ *(right).*

Lecture 3. Goal-oriented error estimation (DWR method)
Lecture 4. Practical aspects

Exercise 5: Discuss the application of the general error representation used in the DWR method in the case of a *linear* variational problem with a likewise *linear* output functional.

Solution: Primal and dual Galerkin approximations of linear problems:

$$\begin{aligned} A(u,\varphi) &= F(\varphi) \quad \forall \varphi \in V, \qquad & A(u_h,\varphi_h) &= F(\varphi_h) \quad \forall \varphi_h \in V_h \\ A(\psi,z) &= J(\psi) \quad \forall \psi \in V, \qquad & A(\psi_h,z_h) &= J(\psi_h) \quad \forall \psi_h \in V_h \end{aligned}$$

Primal solution u, dual solution z:

$$J(u) = A(u,z) = F(z)$$

Primal error $e := u - u_h$, dual error $e^* := z - z_h$ (by Galerkin orthogonality):

$$J(e) = A(e,z) = A(e,e^*) = A(u,e^*) = F(e^*)$$

$$J(e) = A(e, z-\psi_h) = \underbrace{F(z-\psi_h) - A(u_h, z-\psi_h)}_{=:\, \rho(u_h)(z-\psi_h)} \quad \psi_h \in V_h$$

$$F(e^*) = A(u-\varphi_h, e^*) = \underbrace{J(u-\varphi_h) - A(u-\varphi_h, z_h)}_{=:\, \rho^*(z_h)(u-\varphi_h)} \quad \varphi_h \in V_h$$

$$\Rightarrow \qquad J(e) = \tfrac{1}{2}\rho(u_h)(z-\psi_h) + \tfrac{1}{2}\rho^*(z_h)(u-\varphi_h), \quad \varphi_h, \psi_h \in V_h$$

There holds (only valid in the linear case)

$$J(e) = \rho(u_h)(z-\psi_h) = \rho^*(z_h)(u-\varphi_h) = F(e^*)$$

Exercise 6: The *fixed fraction strategy* in a posteriori mesh adaptation refines and coarsens certain fractions X and Y of those cells with largest and smallest indicator values η_K, respectively,

$$\eta_{K_1} \geq \cdots \geq \eta_{K_i} \geq \cdots \geq \eta_{K_N}.$$

Design refining/coarsening strategies by specifying X, Y, such that

a) the number N of cells approximately doubles in each refinement cycle;

b) the number N of cells is approximately kept constant during the refinement process.

Solution: Let N_{old} be the old number of cells, and X and Y the fractions of cells to be refined and coarsened, respectively. Under (bisection-type) refinement, each cell is replaced by 2^d cells, while coarsening merges 2^d cells into one. All other cells remain as they are. The new number of cells is thus

$$N_{\text{new}} = (1 - X - Y + 2^d X + 2^{-d} Y) N_{\text{old}}.$$

a) In order to approximately double the number of cells, we have to choose fractions $0 \leq X, Y \leq 1, X + Y \leq 1$, such that $1 - X - Y + 2^d X + 2^{-d} Y \approx 2$. In 2-D, $X = \frac{1}{3} + \frac{1}{4} Y$ solves this. Usually, $Y = 0$ and thus $X = \frac{1}{3}$.

b) To keep the number of cells roughly constant, $1 - X - Y + 2^d X + 2^{-d} Y \approx 1$ has to hold. In 2-D, the solution of this equation is $X = \frac{1}{4} Y$. Usually, $X = \frac{1}{10}$ and thus $Y = \frac{2}{5}$.

It should be noted that a cell can only then be coarsened if all its child cells are marked for coarsening. In practice, marking a fraction Y of all cells for coarsening will therefore yield much less cells that will actually be unrefined. Thus, the computations above are only an indication for N_{new}.

Exercise 7: Functional-oriented a posteriori error estimates can also be stated in terms of energy-norm error bounds. Consider the Poisson model problem. With the primal and dual errors $e := u - u_h$ and $e^* := z - z_h$, respectively, by Galerkin orthogonality there holds

$$|J(e)| = |(\nabla e, \nabla z)| = |(\nabla e, \nabla e^*)| \leq \|\nabla e\| \, \|\nabla e^*\|.$$

Then, any a posteriori bound for the energy-norm error supplies also a bound for $|J(e)|$. Specify a situation in which this simple minded approach is inefficient. Why is this approach not suited to extract refinement indicators from the error estimate?

Solution: The approach based on energy error estimates for primal and dual solutions is attractive since such estimates are well known and provide a high degree of accuracy. However, consider the point evaluation of the derivative error

$$J(e) := \partial_1 e(a), \quad a \in \Omega.$$

On uniformly refined meshes, there holds $|J(e)| = \mathcal{O}(h)$, for smooth u, and for the singular dual solution z, we only have

$$\|\nabla e\| = \mathcal{O}(h), \quad \|\nabla e^*\| = \mathcal{O}(h^{-1}).$$

On the other hand, on "optimally" refined meshes,

$$|J(e)| = \mathcal{O}(\mathrm{TOL}),$$

and

$$\|\nabla e\| = \mathcal{O}(\mathrm{TOL}^{1/2}), \quad \|\nabla e^*\| = \mathcal{O}(1).$$

In both cases the energy-norm-error-based estimate is of sub-optimal order. Note that we also cannot extract refinement indicators from the estimate, since it cannot be localizes, i.e., the estimate

$$(\nabla e, \nabla e^*) \leq \sum_{K \in \mathbb{T}_h} h_K \|\nabla^2 u\|_K h_K \|\nabla^2 z\|_K$$

does not hold.

Exercise 8 (Practical exercise): Consider the Poisson problem

$$-\Delta u = 1 \text{ in } \Omega, \quad u_{|\partial\Omega} = 0,$$

on the domain $\Omega \subset (-1,1)^2$, shown in the figure below. Compute the function values $u(a)$ and $\partial_1 u(a)$ at the point $a = (.75, .75)$.

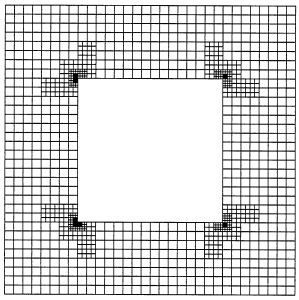

a) Use the provided program for computing $\partial_1 u(a)$ for a sequence of tolerances $\mathrm{TOL}_\mathrm{i} = 4^{-i}$, $i = 1, 2, \ldots$, and monitor the behavior of the true error and the number of cells depending on the achieved accuracy TOL. The code uses the duality-based weighted error estimator described in the lecture and the *fixed error fraction strategy* for mesh refinement.

b) The critical assumption in estimating the efficiency of mesh refinement strategies based on weighted a posteriori error estimates is the "convergence" of residuals, for bilinear finite elements expressed as

$$\|D_h^2 u_h\|_\infty = \max_{K \in \mathbb{T}_h} h_K^{-3/2} \|[\partial_n u_h]\|_K \leq c(\nabla^2 u),$$

if u has uniformly bounded second derivatives, or more locally, for the case that u is not regular (e.g., has corner singularities),

$$|D_h^2 u_{h|K}| := h_K^{-3/2} \|[\partial_n u_h]\|_K \leq c(\max_{\tilde{K}} |\nabla^2 u|),$$

with a cell patch $\tilde{K}$ around K and constants independent of h. The first relation can be proven for quasi-uniform meshes, but is still open for general locally refined meshes including hanging nodes. We want to check these conditions by numerical experiments. Monitor the behavior of $|D_h^2 u_{h|K}|$ for increasingly refined meshes. Try to interpret the observed results.

Solution: a) Figure 3 shows two optimal meshes generated by the weighted error estimator for the functionals $J(u) = u(a)$ and $J(u) = \partial_1 u(a)$, respectively, with $a = (0.75, 0.75)$. Figure 4 shows the quality of error estimation on a sequence of these meshes, where for the evaluation of the error representation the dual solution was approximated by piecewise quadratic finite elements. As can be seen, the error is estimated very well.

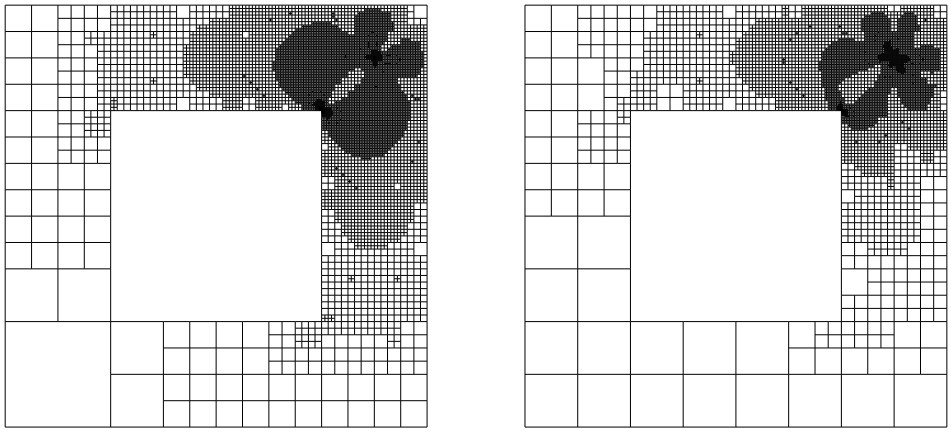

Figure 3: *Meshes after 7 refinement cycles for the point value* $u(a)$ *(left) and the point derivative* $\partial_1 u(a)$ *(right).*

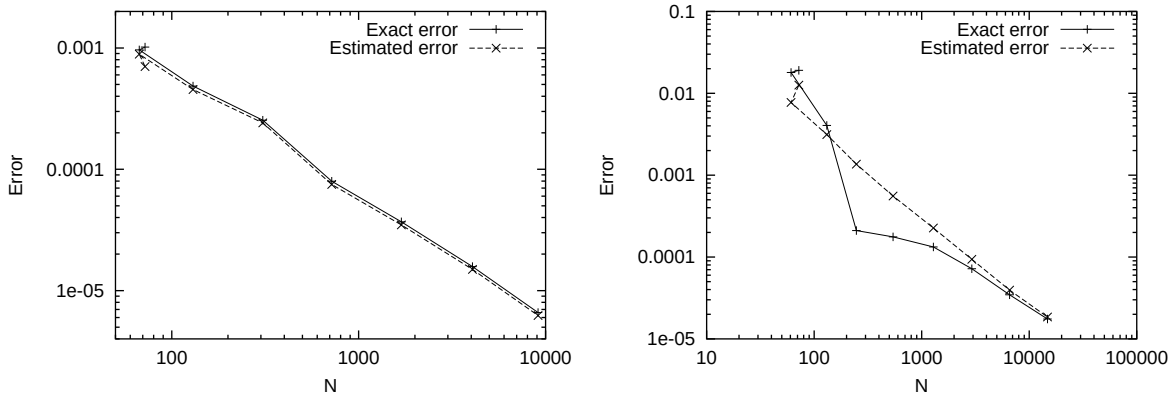

Figure 4: *Quality of error estimates for the point value* $u(a)$ *(left) and the point derivative* $\partial_1 u(a)$ *(right).*

b) For the point value evaluation $J(u) = u(a)$, the convergence behavior of the error is shown in Figure 5 for the following refinement criteria:

- Global refinement.
- Edge residuals: We drop the cell residual term from the error representation formula, and remove the weights involving the dual solution by assuming that there exists an a priori stability estimate for its second derivatives. We are then left with the following cell-wise term: $\eta_K = h_K^{1/2} \|[\partial_n u_h]\|_{\partial K}$.
- Weighted edge residuals: We replace the weights involving the dual solution by an a priori guess on each cell. Since for the point value, $\nabla^2 z$ decays as r^{-2}, where $r = |x-a|$, we take as indicator for refinement the expression $\eta_K = h_K^{1/2} \|[\partial_n u_h]\|_{\partial K} r_K^{-2}$.
- The full dual weighted error estimator η_ω .

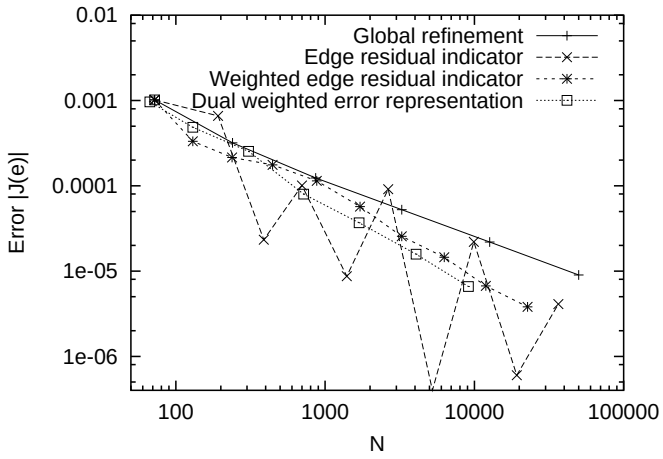

Figure 5: *Comparison of various refinement criteria for computating the point value* $u(a)$.

As can be seen from the figure, a posteriori error indicators do a much better job than global refinement. Using the guessed weight is almost as good as the full weighted error estimator; the difference between the two can probably be attributed to the fact that the weight r^{-2} does not 'see' the singularities of the dual solution at the reentrant corners of the domain, in contrast to the numerically computed approximation

The original edge residual indicator without weights displays a rather irregular behavior. The sign of the error is changing multiply, and the error grows at several refinement steps. The computed values are here, as opposed to the other criteria, not suitable for extrapolation.

Figure 6 shows the primal and dual solutions for the mean-value functional.

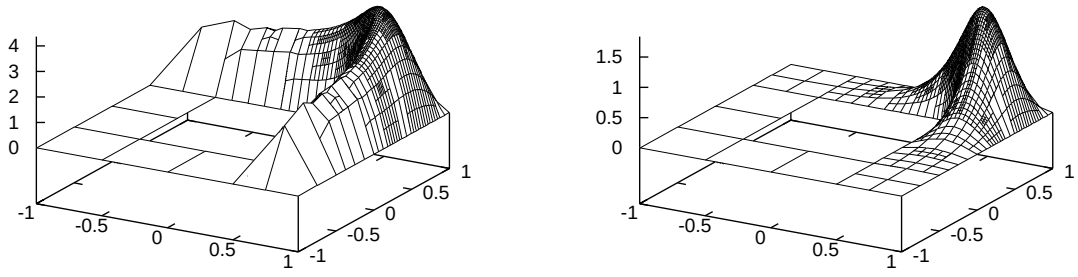

Figure 6: *Primal and dual solutions for the mean-value functional.*

Figure 7 shows the ratio of the nonlinearity indicator $\Delta\rho$ and the (second-order error estimate) $(\rho + \rho^*)/2$. In the left graph, this ratio is shown when primal and dual weights are approximated by a patch-wise higher-order interpolation. The result is a rather small

value of the nonlinearity indicator, much less than 1 per cent even as we approach the critical eigenvalue $\alpha \approx 72.3$ (see also the solution to exercise 7.4).

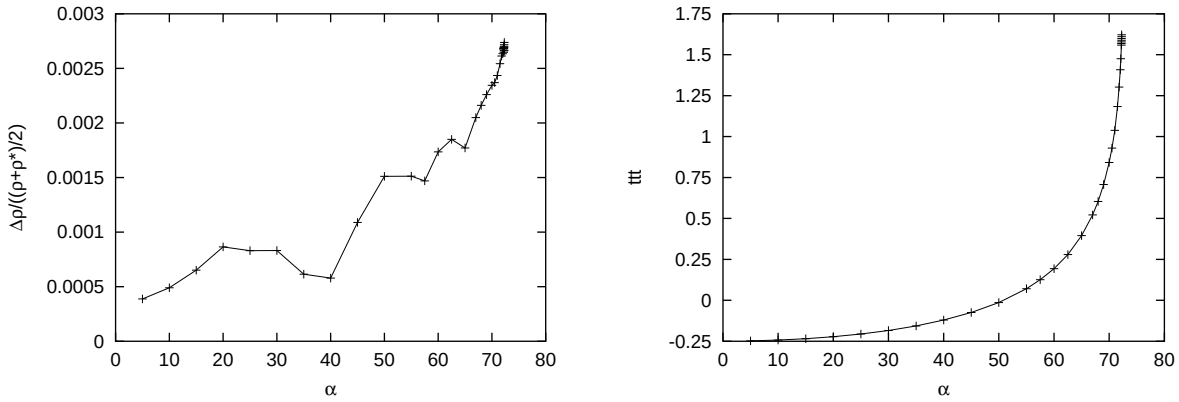

Figure 7: *Ratio* $\Delta\rho/((\rho + \rho^*)/2)$ *between the nonlinearity term and the error estimate. Left: Approximation of primal and dual weights by patch-wise biquadratic interpolation. Right: Approximation of the dual weight by a higher-order Ritz projection. Note the difference in scale.*

However, as the right graph of the figure indicates, the above result is misleading: if the dual solution is approximated by a higher-order Ritz projection, then ρ and ρ^* are no more as close together, and $\Delta\rho$ becomes large, especially as we approach the critical eigenvalue. Close to the critical value, the difference between the two residuals becomes larger than the residuals themselves, making the error estimate quite unreliable.

The interpretation of this is that if both primal and dual weights are approximated using a higher-order interpolation, then the approximated residuals $\tilde{\rho}$ and $\tilde{\rho}^*$ are both not particularly close to the exact error, but the effects of approximation shift their values in the same direction, thus canceling out and pretending a small $\Delta\rho$. On the other hand, when replacing z by its biquadratic Ritz projection, ρ is computed to a high accuracy, while ρ^* is still inaccurate because the weights in this term are only obtained by interpolation. Then, the approximation effect in ρ^* is not canceled by that in ρ, and we obtain a large value for $\Delta\rho$.

In effect, the evaluation of $\Delta\rho$ does not tell us very much in this particular example, if we do not take into account the effects of numerically approximating the weights in the residuals.

Lecture 5. Eigenvalue problems
Lecture 6. Optimization problems
Lecture 7. Time-dependent problems
Lecture 8. Applications in structural mechanics

Exercise 9: Consider the approximation of the Poisson problem

$$-\Delta u = f \quad \text{in } \Omega, \quad u_{|\partial\Omega} = 0,$$

(or the Lamé-Navier equations in linear elasticity) by bilinear finite elements. Develop an a posteriori error estimator and corresponding mesh refinement strategy for controling the maximum norm errors

$$\|u - u_h\|_{L^\infty} \quad \text{or} \quad \|\nabla(u - u_h)\|_{L^\infty}.$$

Solution: (i) We start with the maximum error of $u - u_h$. Let z^a be the dual solution corresponding to any point $a \in \Omega$ satisfying

$$(\nabla\varphi, \nabla z^a) = J^a_\epsilon(\varphi) = \frac{1}{|B_\epsilon(a)|}\int_{B_\epsilon(a)} \varphi(x)\,dx, \quad \forall\varphi \in H^1_0(\Omega),$$

with regularization $\epsilon = TOL$. For smooth u, we have (for any location of the point a, even close to the boundary)

$$J^a_\epsilon(u) = u(a) + \mathcal{O}(TOL).$$

Then, by the general (linear) theory,

$$|J^a_\epsilon(e)| \le c_I \sum_{K\in\mathbb{T}_h} h^4_K \rho_K(u_h)\omega^a_K,$$

where

$$\rho_K(u_h) := \max_K |f + \Delta u_h| + h_K^{-1} \max_{\partial K} |[\partial_n u_h]|, \qquad \omega^a_K := \max_K |\nabla^2 z^a|$$

This can be converted into the estimate

$$|J^a_\epsilon(e)| \le c_I \max_{K\in\mathbb{T}_h}\{h^2_K\rho_K(u_h)\}\int_\Omega |\nabla^2 z^a|\,dx$$

Recalling the structure of the regularized Green functiuon z^a,

$$|\nabla^2 z^a(x)| \approx (|x-a|^2 + \epsilon^2)^{-1},$$

we have

$$\int_\Omega |\nabla^2 z^a|\,dx \le c|\log(\epsilon)| \approx |\log(TOL)|.$$

Takin now the maximum over $a \in \Omega$, the final result is

$$\|u - u_h\|_{L^\infty} \le c|\log(TOL)| \max_{K\in\mathbb{T}_h}\{h^2_K\rho_K(u_h)\} + cTOL.$$

(ii) In an analogous way, we may derive the estimate

$$\|\nabla(u - u_h)\|_{L^\infty} \le c|\log(TOL)| \max_{K\in\mathbb{T}_h}\{h_K\rho_K(u_h)\} + cTOL.$$

Exercise 10: Consider the model convection-diffusion eigenvalue problem

$$-\Delta v + b \cdot \nabla v \;=\; \lambda v \quad \text{in } \Omega, \quad \mathrm{v}_{|\partial\Omega} = 0.$$

Under the assumption that the eigenfunctions have H^2-regularity, and that

$$|(u-u_h, u^*-u_h^*)| \le 1,$$

prove the a posteriori error bound

$$|\lambda-\lambda_h| \;\le\; \eta_\lambda^{(2)} := c_\lambda \Big(\sum_{K\in\mathbb{T}_h} h_K^4 \big\{ \rho_K^2 + \rho_K^{*2} \big\} \Big)^{1/2},$$

with a constant $c_\lambda = \mathcal{O}(|\lambda|)$.

Solution: We recall the estimate

$$|\lambda-\lambda_h| \le \eta_\lambda^\omega := \sum_{K\in\mathbb{T}_h} \big\{ \rho_K \omega_K^* + \rho_K^* \omega_K \big\},$$

$$\begin{aligned}
\rho_K &:= \big(\|R_h\|_K^2 + h_K^{-1} \|r_h\|_{\partial K}^2 \big)^{1/2}, \\
\rho_K^* &:= \big(\|R_h^*\|_K^2 + h_K^{-1} \|r_h^*\|_{\partial K}^2 \big)^{1/2} \\
\omega_K^* &:= \big(\|u^*-I_h u^*\|_K^2 + h_K \|u^*-I_h u^*\|_{\partial K}^2 \big)^{1/2}, \\
\omega_K &:= \big(\|u-I_h u\|_K^2 + h_K \|u-I_h u\|_{\partial K}^2 \big)^{1/2}.
\end{aligned}$$

It remains to estimate the weights ω_K and ω_K^*. By the usual estimates for the nodal interpolations $I_h u$ and $I_h u^*$, we have

$$\omega_K^* \le c_I h_K^2 \, \|\nabla^2 u^*\|_K, \qquad \omega_K \le c_I h_K^2 \, \|\nabla^2 u\|_K.$$

This gives us the intermediate result

$$|\lambda-\lambda_h| \le c_I \Big(\sum_{K\in\mathbb{T}_h} h_K^4 \rho_h^2 \Big)^{1/2} \|\nabla^2 u^*\| + c_I \Big(\sum_{K\in\mathbb{T}_h} h_K^4 \rho_h^{*2} \Big)^{1/2} \|\nabla^2 u\|.$$

Since u and u^* are eigenfunctions of the operators $\mathcal{A} := -\Delta + b\cdot\nabla$ and $\mathcal{A}^* := -\Delta - b\cdot\nabla$, respectively, there holds

$$\|\nabla^2 u\| + \|\nabla^2 u^*\| \le c_1(\mathcal{A}) \big\{ \|\mathcal{A} u\| + \|\mathcal{A}^* u^*\| \big\} = c_1(\mathcal{A}) |\lambda| \, \{ \|u\| + \|u^*\| \},$$

with some constant $c_1(\mathcal{A})$. Since $\|u^*\| \le c_2(\mathcal{A})$, the asserted estimate follows.

Exercise 11: The solution of the elliptic eigenvalue problem

$$-\Delta u = \lambda u \ \text{ in } \Omega, \quad u_{|\partial\Omega} = 0,$$

can be reformulated in the context of parameter estimation as follows:
Minimize

$$J(u) := \tfrac{1}{2}(u-1,1)^2 \ \to \ 0,$$

for pairs $\{u,\lambda\} \in H_0^1(\Omega) \times \mathbb{R}$ satisfying

$$(\nabla u, \nabla\psi) = \lambda(u,\psi) \quad \forall \psi \in H_0^1(\Omega).$$

Following the Euler-Lagrange approach, formulate the first-order necessary condition for computing the first (simple) eigenvalue $\lambda_{\min} > 0$ and show that in this case the adjoint solution vanishes, i.e., $z \equiv 0$. This shows that for guiding mesh refinement in computing eigenvalues another approach has to be used. We remark that, here, the cost functional $J(u)$ contains the *linear* normalization condition $(u,1) = 1$ which is an alternative to the usual *quadratic* normalization condition $\|u\|^2 = 1$.

Solution: The Lagrangian for this problem reads

$$L(u,\lambda,z) = J(u) - A(u)(z) = \tfrac{1}{2}(u-1,1)^2 - (\nabla u, \nabla z) + \lambda(u,z).$$

From this, we obtain the optimality conditions determining a solution to the constrained optimization problem:

$$\begin{aligned}
L'_u(u,\lambda,z)(\varphi) &= (u-1,1)(\varphi,1) - (\nabla\varphi,\nabla z) + \lambda(\varphi,z) = 0,\\
L'_\lambda(u,\lambda,z)(\mu) &= (u,z) = 0,\\
L'_z(u,\lambda,z)(\psi) &= -(\nabla u,\nabla\psi) + \lambda(u,\psi) = 0,
\end{aligned}$$

for all test functions $\{\varphi,\mu,\psi\}$. In strong form, the first and last equations read

$$-\Delta u - \lambda u = 0, \quad -\Delta z - \lambda z = (u-1,1).$$

The first determines the eigenvalue λ and the eigenfunction u up to a multiplicative constant. Since the second optimality condition above requires that z has no component in direction of u, this removes the kernel of the operator $-\Delta-\lambda$, using the assumption of simplicity of this eigenvalue. Furthermore, the adjoint equation has a solution only if the right hand side (which is a constant) is in the range of the operator, $\mathcal{R}(-\Delta-\lambda) = \mathcal{N}(-\Delta-\lambda)^\perp = \{u\}^\perp$; this condition is only satisfied if either the constant right hand side is zero, or if u has mean value zero. Since it is known that the lowest eigenfunction of the Laplacian does not change its sign, the second case cannot occur. In the first case, u is normalized, and the solution of the adjoint equation is necessarily $z \equiv 0$. Since in the error representation formula all terms contain z multiplicatively, the error is zero, for every grid chosen.

The reason for this surprising behavior is that we have set out to control the error in the functional $J(u) = \frac{1}{2}\{(u,1)-1\}^2$. For the exact minimizer, $J(u) = 0$. On the other hand, we can find discrete eigenvalue/eigenvector pairs on *every* grid, and can normalize the eigenvector to $(u_h,1) = 1$. So $J(u_h)$ can be made equal to zero as well on each grid, making $J(u)-J(u_h) = 0$. Thus, the error estimator only tells us that we can make the error in this quantity to zero on every grid.

Lecture 9. Applications in fluid mechanics
Lecture 10. Miscellaneous and open problems

Exercise 12 (Concluding discussion): Complete the preceding practical exercises and summarize the observed results. In the executed tests with bilinear finite elements, we made the following observations:

- **Tests on the square domain:**
  (i) On sequences of uniformly refined meshes derivative point values and normal flux integrals converge with order $\mathcal{O}(h^2)$, which ist due to "super-approximation". This corresponds to the complexity $N \approx TOL^{-1}$. On unstructured meshes the order would be only $\mathcal{O}(h)$. Putting in randomly distributed cells with hanging nodes significantly reduces the accuracy.
  (ii) The adaptive computation of the local quantities by using the DWR method achievesn the predicted (optimal) order $N \approx TOL^{-1}$ with a constant significantly better than that for the case of uniformly refined meshes.
  (iii) On the locally refined meshes the second-order difference quotients (scaled normal-jump cell boundary integrals) of the discrete solutions stay bounded, which supports the corresponding assumption in the theoretical analysis for the DWR method.

- **Tests on a square domain with a square hole:**
  The efficiency of the computation of derivative point values using the DWR method is significantly better than that of driving the mesh adaptation by "regularity-based" strategies or on uniformly refined meshes.

Conclusion: *The DWR method works according to the theoretical predictions.*